Geology and Petrology of the Nishi and Fudenzaki Formations of the Aguni Group, Aguni Island, the Central Ryukyu Arc : Petrogenetic Relationship between the Andesites and Dacites

Bull. Coll. Sci., Univ. Ryukyus, No. 60 : 27 - 50 (1995)

Geology and Petrology of the Nishi and Fudenzaki Formations of the Aguni Group, Aguni Island, the Central Ryukyu Arc: Petrogenetic Relationship between the Andesites and Dacites

Ryuichi SHINJO*, Ken USAMI*, and Yuzo KATO*

* Department of Marine Sciences, University of the Ryukyus, Senbaru 1, Nishihara, Okinawa 903-01, Japan

Abstract

The late Miocene volcanic rocks of the Aguni Group range from basalt to rhyolite, and have a pronounced compositional gap between 57 and 69 wt.% SiO_2. Sr isotopic ratios for a dacite lava from the Nishi Formation (0.70463) and a gabbroic fragment from the Fudenzaki Formation (0.70455) are similar to those of the basalt-andesite suite (0.70452-0.70466). Both major- and trace-element variations from andesite to dacite are explainable in terms of fractional crystallization involving removal of the observed phenocryst phases in the evolved volcanic rocks. The Rare Earth Elements (REE) patterns of gabbroic fragments appear to coincide with the pattern of cumulate expected from fractional crystallization. A shallow composition-temperature slope of cotectic involving amphibole-bearing gabbroic assemblages is responsible for the development of bimodality between the andesites and dacites.

Introduction

Late Miocene volcanic rocks (Aguni Group) and Quaternary limestone (Doji Formation) form Aguni Island in the central Ryukyu arc (Fig. 1). The Auguni Group has been divided into three formations: Nishi, Fudenzaki, and Higashi Formations. Shinjo *et al.* (1990) described the geology and petrology for the Higashi Formation, whereas the petrological feature of the Nishi and Fudenzaki Formations remain unclear. The Fudenzaki Formation includes various types of ultramafic to felsic fragments and crustal rocks (Kato, 1985). Some of them appear to be genetically related to their host rocks. The volcanic rocks in the Aguni Group range from basalts and andesites, to dacites and rhyolites, representing a wide range of major- and trace-elements. In addition to geology of the Fudenzaki Formation, this paper presents whole-rock chemistry and Sr-isotopic composition of the volcanic rocks and gabbroic fragments from the Nishi and Fudenzaki Formations. Utilizing data from this investigation and from results of Shinjo *et al.* (1990), we present a petrogenetic model on the volcanic rocks of the Aguni Group.

Geology

Aguni Island (127°14E', 26°35'N) is in the central Ryukyu arc and is 60 km west of Okinawa Island (Fig. 1). The island lies west of a convergent margin along the Ryukyu trench, where the Philippine Sea plate has been actively underthrusting the continental Eurasian plate.

Kamiya (1973) described the geology of Aguni Island. Recent mapping on the island has been undertaken by Kato (1985). Figure 1 shows the geological map of Aguni Island.

Accepted : July 10, 1995

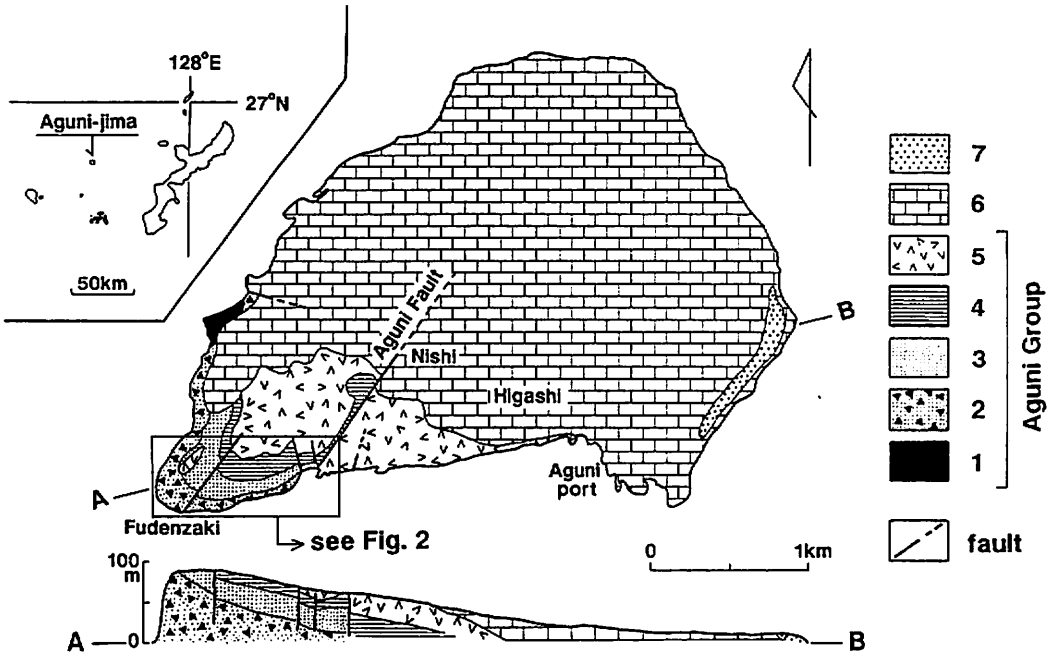

Fig. 1. Generalized geological map of Aguni Island (after Kato, 1985). 1, Nishi Formation; 2-4, Fudenzaki Formation; 2, A Member; 3, B Member; 4, C Member; 5, Higashi Formation; 6, Quaternary Doji Formation (Ryukyu Limestone); 7, Dune sand.

The island is made up of late Miocene volcanic rocks (Aguni Group) and Quaternary limestone (Doji Formation). The Doji Formation overlies unconformably on Aguni Group, covers a broad area of the island, and constructs a flat terrain. On the basis of the submarine geophysical survey, Ujiié (1983) suggested that the surrounding area of Aguni Island is consist with late Miocene - Pliocene volcanic basements. Thus, the island is considered to be a remnant of large volcanic edifices. The highest peak on the island is 97.3 m near the cape Fudenzaki. It's elevation decreases gently toward the northwest.

The Aguni Group has been divided, in ascending order, into three Formations: Nishi, Fudenzaki, and Higashi Formations. The Nishi Formation is composed of a single dacite lava flow, over 30 m thick, which is exposed in a limited area in the northwest of the island. A dacite of the Nishi Formation is dated at 6.24 ± 0.46 Ma (Fission track age: Daishi *et al.*, 1986).

The Fudenzaki Formation overlies on the Nishi Formation. Detailed distributions and columnar sections of the Fudenzaki Formation are shown in Fig. 2. On the basis of the lithological characteristics, the formation has been subdivided, in ascending order, into three members: A, B, and C Members. Each contact between the members is conformable.

The A Member unconformably overlies a dacite lava flow of the Nishi Formation, and consist of white pumiceous tuff breccia. The member is well exposed on the cliff at Cape Fudenzaki (Fig. 3a). Thickness of the A Member is over 65 m, and gradually declines toward the east. We interpret this member as being as pumice flow deposits. A layer of volcanic breccia, 2 to 3 m thick, is intercalated at the middle portion of the member (Figs. 3a and 3b). This member carries abundant xenoliths and cognate fragments, which vary

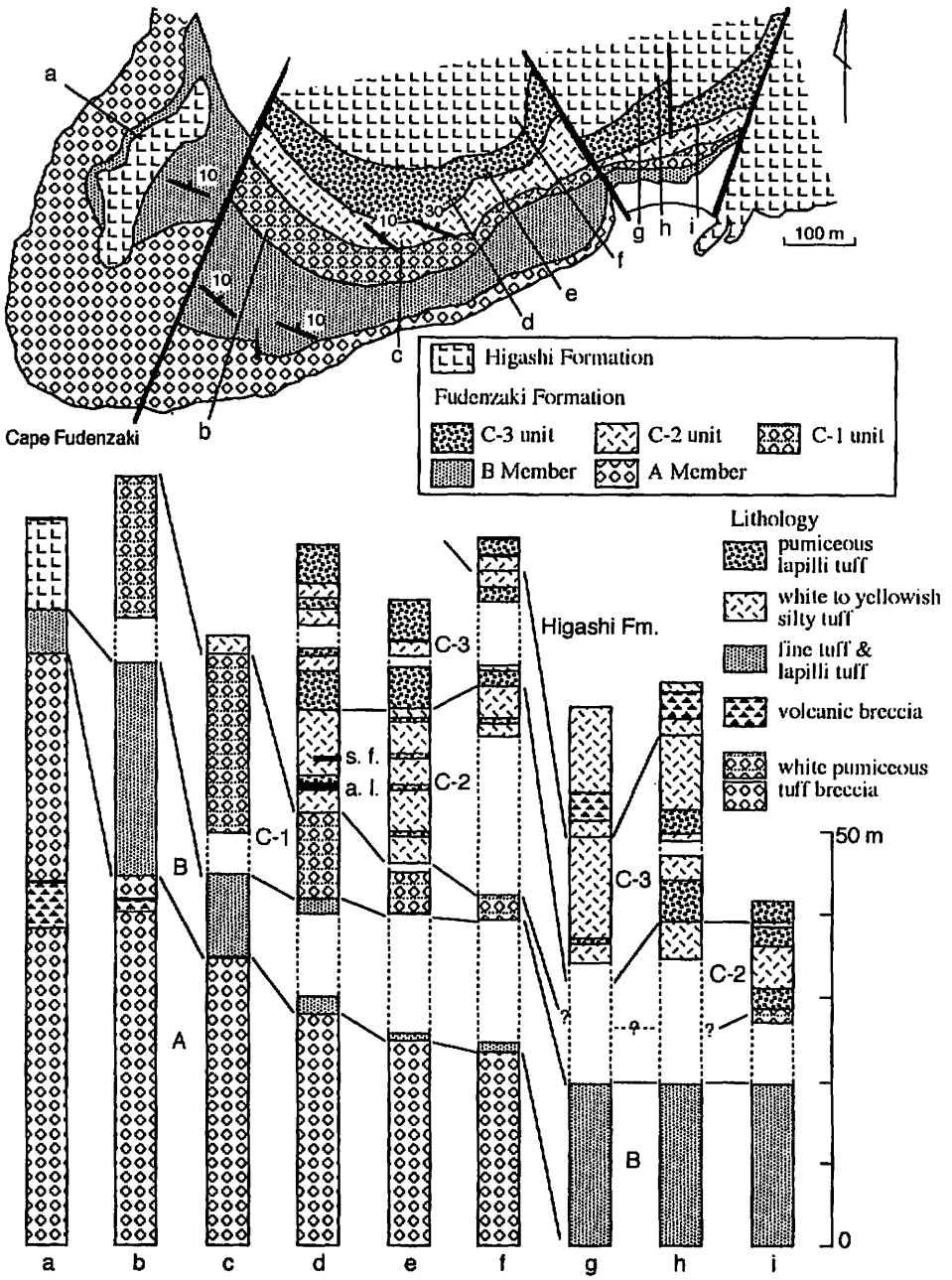

Fig. 2. Geological map and columnar sections of the Fudenzaki Formation. Accretionary lapilli layer (a. l.) and shell fossil-concentrated zone (s. f.) occur in the middle position of C-2 unit.

from few to several tens of centimeters in size.

The B Member is mainly composed of alternations every few centimeters of pumiceous lapilli tuff and white fine tuff. Thickness of the B Member is about 20 m, and gradually thickens toward the east. General attitude is N70° W strike and 10° NE dip. They are

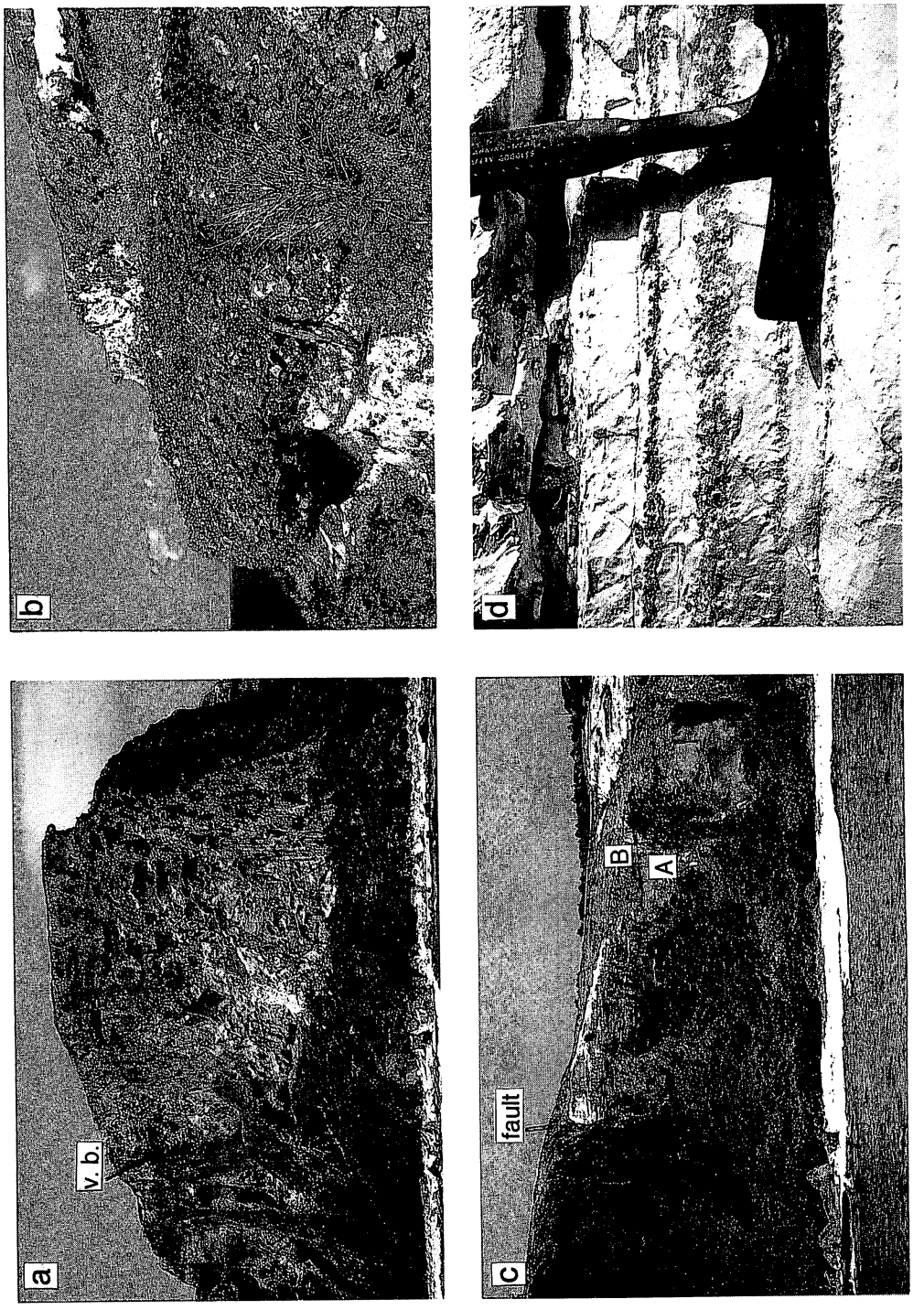
a
v. b.
b
c
fault
B
A
d

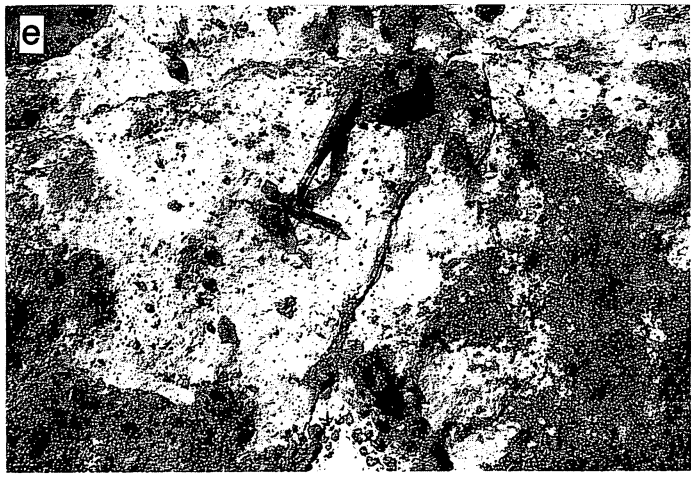

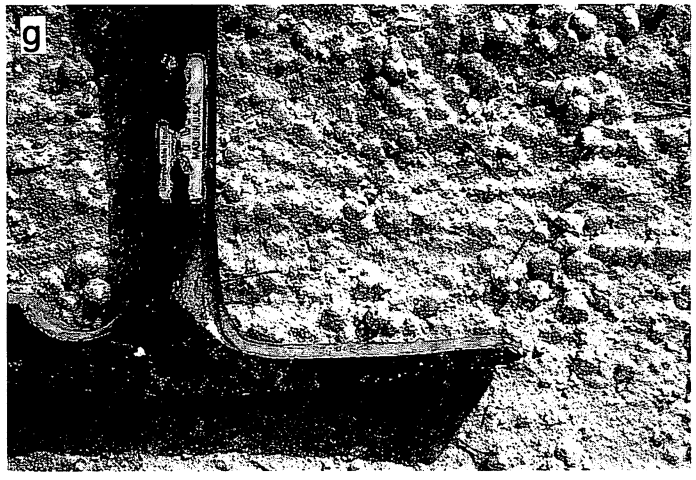

Fig. 3a-g. (a) Outcrop of the A Member, Fudenzaki Formation at cliff near Cape Fudenzaki. A layer of volcanic breccia (v. b.) is in the upper portion. (b) Close-up of the volcanic breccia in the A Member. (c) Well-stratified B Member (B) overlies on the A Member (A). (d) An alternation of white fine tuff and pumiceous lapilli tuff of the B Member. (e) White pumiceous tuff breccia in the C-1 unit, which carries abundant dark cognate fragments and xenoliths. (f) An alternation of yellowish silty tuff and white fine tuff in the C-2 unit, which includes a layer of accretionary lapilli (a. l.). (g) Close-up of an accretionary lapilli layer.

commonly crossbedded at the lower position in the member, indicating that they deposited in a subaqueous environment.

The C Member, 40 to 45 m thick, is underlain unconformably by an andesitic lava and breccia of the Higashi Formation at near the Cape Fudenzaki. Thickness of the C Member gradually declines toward the east. The C Member is further subdivided, in ascending order, into three units, which have been named C-1, C-2, and C-3 units. The C-1 unit lacks layered structure and has similar lithology to the A Member (Fig. 3e). The outcrop is restricted at an area from the light house on Fudenzaki to the east about 500 m. This unit contains abundant cognate rock fragments and xenoliths, as does the A Member. The C-2 unit consists of an alternation of white fine tuff and yellowish silty tuff. The outcrop is limited, but is present at about 250 m east of the light house on Fudenzaki. Thickness of this unit is 10 to 15 m. The unit strikes N 65° W and dips north. The unit contains an intercalated accretionary lapilli layer, 50 cm thick, which is exposed about 300 m east of the light house on Fudenzaki and is in the mid-portion of the unit (Fig. 3f). Accretionary lapillis are generally 5 mm in diameter (Fig. 3g). We recognized a fossil zone of shell in the yellowish silty tuff, which crops out slightly upper position of the accretionary lapilli layer. The C-3 unit, about 20 m thick, is composed of white to yellowish silty tuff, with persistent white pumiceous lapilli tuff.

The Higashi Formation consists of lava flows, breccias, and pyroclastic rocks of basalt to andesite composition. Details of this formation were described by Shinjo *et al.* (1990). They subdivided the Higashi Formation into two units, the lower and upper units. The lower unit includes basaltic lavas, whereas the upper unit is composed of andesite lavas and pyroclastics.

Analytical procedures

Major- and trace-element whole-rock compositions were obtained by X-ray fluorescence (XRF) analysis at Tohoku University according to the procedures of Fujimaki and Aoki (1980). Rare earth elements (REEs), Y, and Sc are separated from unwanted elements by using conventional ion-exchange techniques, and are determined by Inductively Coupled-Plasma Mass Spectrometry (ICP-MS) at University of the Ryukyus. Standard rocks GSJ JB-1 and JA-1 were prepared as standards. Strontium isotopic data were obtained on the Finnigan MAT 261™ mass spectrometer at Tohoku University using procedures described by Fujimaki *et al.* (1992). $^{87}Sr/^{86}Sr$ are normalized to $^{86}Sr/^{88}Sr=0.1194$. We obtained $^{87}Sr/^{86}Sr = 0.710236 \pm 0.000020$ (2σ mean) for NBS SRM-987.

Petrography and mineralogy

Table 1 shows a summary of the mineralogy of dacite lava, essential pumice clasts, and tuff from the Nishi and Fudenzaki Formations, as well as the fresh cognate fragments that are included in the Fudenzaki Formation. The fresh pumice clasts are collected from the Fudenzaki Formation. Representative mineral compositions are given in the Appendix.

The dacite lava of the Nishi Formation is porphyritic, with about 35 % modal phenocrysts set in hyalopilitic groundmass. The phenocryst (microphenocryst) assemblage is plagioclase (Plag) + hornblende (Hbl) + orthopyroxene (Opx) + magnetite (Mt). Phenocrysts are subhedral to euhedral, and less than 2 mm in size. Orthopyroxene is present only as a microphenocryt. Crystal clots of Plag + Hbl + Mt were rarely observed.

Table 1. Summary of mineralogy of volcanic rocks and rock fragments from the Nishi and Fudenzaki Formations.

Sp. No.	rock type	Phenocryst and microphenocryst							Member
		Qtz	Plag	Cpx	Opx	Amph	Bt	Opq	
Nishi Formation: lava									
AG-DA*	dacite		XXX		X	XX		X	
Fudenzaki Formation: pumice & tuff									
AG23	tuff	X	XXX		X	XXX			C-3
AG30	tuff	X	XX		X				C-2
AG28	tuff	X	XX			XX			C-2
AG12	tuff	X	XXX		XX	X		XX	C-1
AG25*	pumice	X	X		X			X	C-1
AG8	tuff	X	XXX		XX	X		XX	A
AG24*	pumice		XXX		X	XX		X	A
Cognate rock fragments in Fudenzaki Formation									
AG66*	andesite		XXX	XX				X	C-1
AG59	andesite		XXX	XX				X	A
AG60	andesite		XX	X	X				A
AG10U*	dacite		XXX		XX				A
AG11*	dacite		XXX		XX	X	X	X	A
AG34	dacite	X	XXX			X		X	C-1
AG72	dacite		XXX	X		X			C-1
AG52	dacite	X	XXX			XXX		X	A
AG53	dacite		XXX		X	X		X	A
AG57	rhyolite	X	XXX				X	XX	A
AG61	rhyolite		XX	X					A
AG65	obsidian	X	X						C-1
AG69*	obsidian		XXX		XX	XX		X	C-1
AG46	obsidian	X	XXX	X	X	X		X	A
AG49	obsidian		XXX		XX	X			A
AG68	perlite		XXX	X	XX	X		X	C-1
AG48*	perlite	X	X		X	X		X	A
AG47*	gabbro		XXX	XXX		X		X	A
AG51*	gabbro		XXX	XX		XXX		XX	A
AGXGB*	gabbro		XXX	X		XXX		X	A

Modal mineralogy is indicated by XXX, XX, and X in order of abundance.

* Samples analyzed for whole-rock chemical compositions.

The pumice clasts in the Fudenzaki Formation are generally aphyric, containing less than 5% modal phenocrysts. The phenocryst assemblage in pumice and tuff is generally similar to those in dacite of the Nishi Formation, but includes comparatively few quartz (Qtz).

The Fudenzaki Formation, A Member and C-1 unit of C Member, contain the various types of rock fragments. These fragments are cognate fragments and xenoliths. The fresh cognate fragments of dacite, rhyolite, obsidian, and perlite have similar mineralogy to those of their host tuff and pumices (Table 1), but they rarely contain phenocrysts of clinopyroxene (Cpx) and biotite (Bt). We interpret the gabbroic fragments to be cognate, as discussed in a later section. Three types of gabbro are recognized (Table 1). The first type (AG47) is coarse-grained amphibole (Amph)-bearing gabbro, which is surrounded by light gray fine-grained quenched rind. The second type (AG51) is Px-Hbl-gabbro, with fine-grained interstitial groundmass with abundant glasses. The third type (AGXGB) is Cpx-bearing Hbl-gabbro, which lacks interstitial groundmass.

Xenoliths are altered volcanic rocks, granitic rocks, and amphibolite. Altered volcanic rocks are greenish in color and have similar lithology to middle Miocene Green Tuff volcanic rocks of the Aradake Formation on Kume Island (Shinjo and Kato, 1988). The

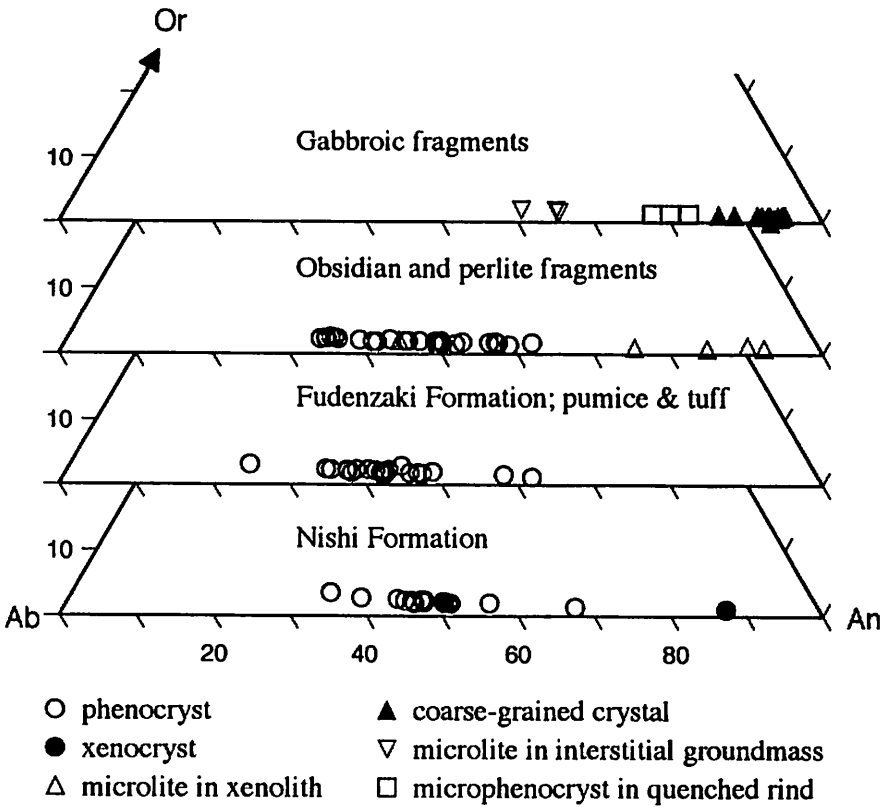

Fig. 4. Plagioclase composition plotted in part of the Or-Ab-An diagram (mol per cent).

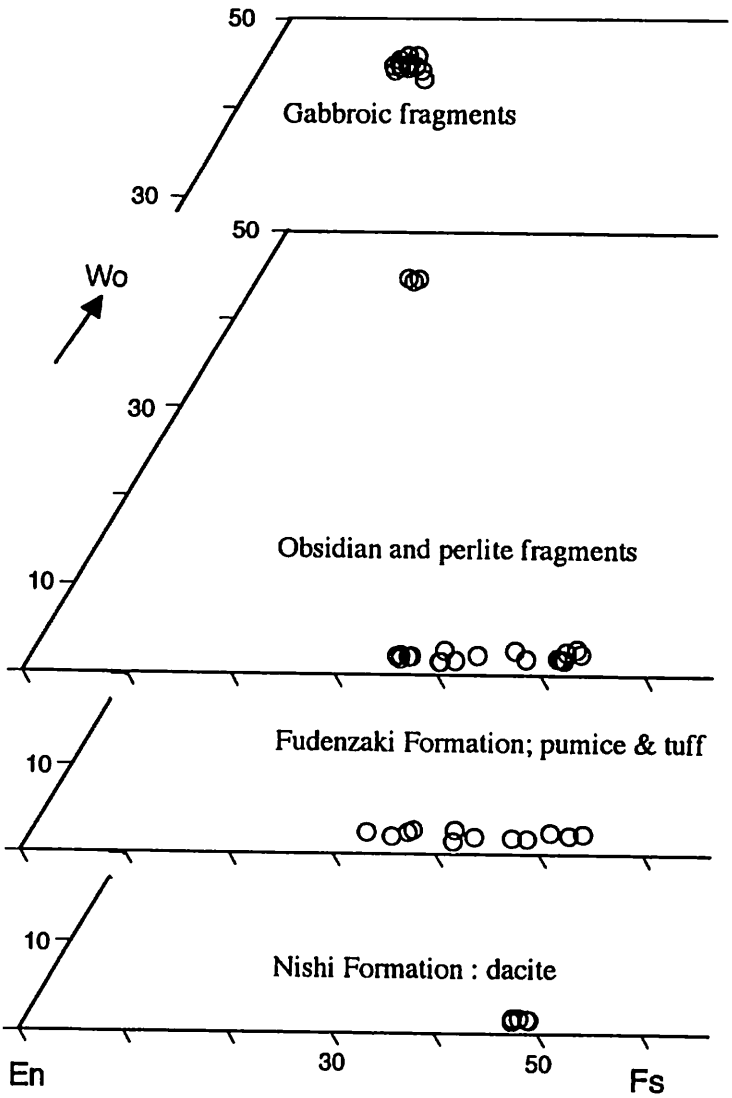

Fig. 5. Pyroxene composition plotted in part of the Ca-Mg-Fe (Wo-En-Fs) quadrilateral.

granitic xenoliths are slightly altered and either granite or granodiorite. They are medium grained and have mineral assemblages composed of Qtz + alkali feldspar (K-fel) + Plag + Amph + Fe-Ti oxide ± Bt. Amphibolite (Amph + Opx) xenolith is very rare. The amphibolite has a weakly foliated structure, and includes small plagioclase sporadically.

Plagioclases: The composition of plagioclases are shown in Fig. 4. Plagioclase phenocrysts in a dacite from the Nishi Formation range from An_{67} to An_{34}, except one grain, which appears to be xenocrystal, having a dusty rounded core of An_{87} and thin clear rim of An_{49}. Phenocrysts in pumices and tuffs in the Fudenzaki Formation range from An_{61} to An_{23}, while most phenocrysts are in the range $An_{49\text{-}34}$. Phenocryst composition in obsidian and perlite fragments concentrate between An_{61} and An_{33}. Plagioclases in the gabbroic

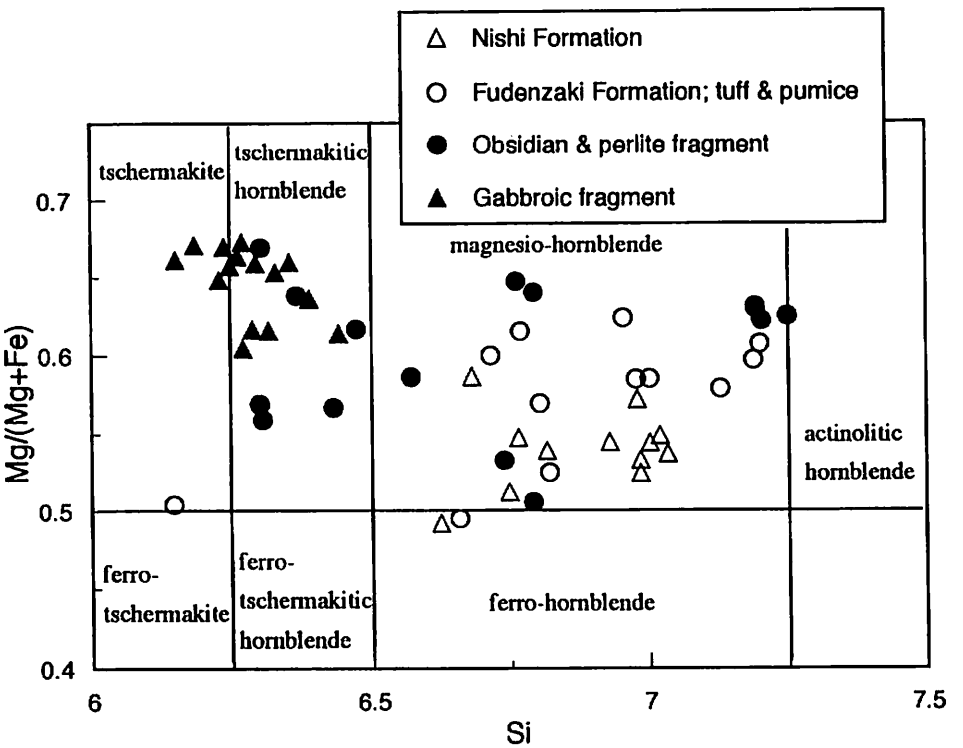

Fig. 6. Composition of amphiboles: atomic Si versus Mg/(Mg+Fe) ratios (nomenclature after Leake, 1968).

fragments have compositions of An_{95}-An_{86} for coarse-grained crystals, An_{65}-An_{60} for microlites in interstitial groundmass, and An_{82}-An_{77} for microphenocrysts in quenched rind.

Pyroxenes: Composition of pyroxenes are illustrated in Fig. 5. The orthopyroxene phenocrysts in a dacite of the Nishi Formation are hypersthene ($Wo_{2\text{-}1}En_{52\text{-}50}$). Phenocryst compositions of orthopyroxene in pumice and tuff of the Fudenzaki Formation are in the range $Wo_{3\text{-}2}En_{65\text{-}45}$. Orthopyroxenes in obsidian and perlite fragments have similar composition ($Wo_{3\text{-}2}En_{63\text{-}45}$) to those of pumice and tuff in the Fudenzaki Formation. Clinopyroxenes in obsidian and perlite are augites with restricted composition ($Wo_{45}En_{41\text{-}40}$) Clinopyroxenes in the gabbroic fragments are also augites and are in the range $Wo_{43\text{-}46}$ $En_{43\text{-}40}$.

Amphibole: Amphibole phenocrysts in dacite from the Nishi Formation and pumice and tuff from the Fudenzaki Formation have similar composition. Most of them are magnesio-hornblende, according to Leake's (1978) nomenclature. Amphibole phenocryst in perlite and obsidian fragments has a wider range of composition. Some of them are similar in composition to those in gabbroic fragments. Amphiboles in the gabbroic fragments are either tschermakitic hornblende or tschermakite. There are no marked differences in composition among the three types of gabbros.

Whole-rock chemistry

Major- and trace-element analytical results are presented in Table 2, together with Sr

isotopic data. All the available data on major elements of the Aguni Group are plotted on silica variation diagrams (Figs. 7 & 8). EPMA glass analyses for pumice, tuff, obsidian, and perlite in the Fudenzaki Formation are given in Table 3, and shown in Fig. 7. The volcanic rock suite of the Aguni Group belong to a high-alumina basalt series (Kuno, 1968),

Table 2. Major and trace element composition and Sr isotopic data for the volcanic rocks and gabrroic fragments in the Aguni Group.

	Nishi Fm.	Fudenzaki Formation										Higashi * Formation	
		cognate rock fragment											
	dac	pum	pum	obs	perl	dac	dac	and	gabbr	gabbr	gabbr	bas	and
Mbr.		A	C-1	A	C-1	A	A	C-1	A	A	A		
Sp. No	AG-DA	AG24	AG25	AG48	AG69	AG10U	AG11	AG66	AG47	AG51	AGXGB	AG406	AG10
SiO_2	69.09	69.20	76.19	76.15	72.03	72.87	71.18	56.41	40.70	39.79	41.95	51.19	56.70
TiO_2	0.46	0.46	0.19	0.19	0.33	0.25	0.29	1.11	1.93	2.72	2.64	1.15	1.03
Al_2O_3	16.35	17.04	12.59	12.79	14.79	14.18	14.34	19.05	17.22	17.13	19.85	18.76	18.62
FeO tot	3.35	3.42	1.56	1.50	2.17	2.21	2.83	7.65	17.26	16.91	12.62	9.96	8.87
MnO	0.08	0.09	0.06	0.06	0.07	0.07	0.08	0.13	0.14	0.15	0.18	0.17	0.17
MgO	0.89	1.10	0.22	0.18	0.60	0.35	0.38	2.88	6.06	8.81	7.55	4.72	2.63
CaO	3.40	2.35	1.21	1.23	2.57	2.01	2.16	7.41	15.58	12.38	13.39	10.43	7.30
Na_2O	4.02	3.77	3.61	4.64	4.60	4.61	5.35	4.05	0.96	1.76	1.61	3.09	3.51
K_2O	2.25	2.56	4.35	3.24	2.80	3.40	3.32	1.15	0.13	0.33	0.19	0.43	1.02
P_2O_5	0.11	0.02	0.02	0.02	0.04	0.05	0.06	0.17	0.02	0.02	0.01	0.10	0.14
LOI	-	5.37	4.24	2.38	2.31	2.93	0.24	0.87	-	0.36	-	-	-
XRF analyses; ppm													
Nb	5.4	6.8	6.0	6.3	5.4	6.3	6.7	5.0	0.7	1.4	3.0	3.6	4.9
Zr	164	215	137	141	140	181	202	145	24	31	27	79	120
Y	27	36	24	24	20	26	40	39	15	28	23	28.3	33
Sr	219	165.0	94	95	177	139	148	221	237	222	253	237	235
Rb	105.1	62.7	86.4	89.6	75.5	109.2	101.5	22.9	3.3	4.0	6.0	8.1	27.2
Th	11.4	6	7	8	7	10	9	-	-	-	-	2.3	3.9
Pb	13.2	13.2	15.9	16.5	13.9	15.1	14.2	9.0	3.2	3.8	-	4.0	5.1
Ni	<1	3	3	3	3	3	3	4	4	-	18	7	<1
Co	4	3	-	-	1	1	2	20	53	60	-	36	19
Cr	8	5	6	8	7	9	8	6	-	-	-	39	7
Ce	48	38	47	43	40	48	50	27	-	6	-	16	25
V	55	29	11	7	27	12	12	167	1028	908	523	288	210
Ba	343	376	449	454	409	379	362	113	25	49	-	74	142
ICP-MS analyses													
Sc	9.1	10.2		3.9		3.9		25.2		117.0	23.1	12.7	37.6
Y	26.1	34.6		22.5		24.9		40.5		26.9	30.2	27.9	34.9
La	18.921	20.384		20.581		20.506		10.927		1.607	1.200	5.176	9.543
Ce	39.648	31.855		40.268		42.600		22.357		5.278	4.203	13.630	22.361
Pr	4.408	4.930		4.229		4.599		3.329		0.969	0.945	1.925	3.079
Nd	17.467	20.933		15.543		17.380		15.728		6.184	6.517	9.723	14.604
Sm	3.545	4.297		2.926		3.323		4.245		2.509	2.868	2.877	3.825
Eu	0.857	1.014		0.589		0.751		1.409		0.932	1.153	1.001	1.246
Gd	3.516	4.381		2.874		3.266		4.887		3.344	3.912	3.334	4.293
Tb	0.591	0.723		0.483		0.550		0.922		0.674	0.803	0.650	0.801
Dy	3.380	4.212		2.798		3.158		5.517		4.136	4.933	3.949	4.710
Ho	0.738	0.951		0.624		0.699		1.217		0.877	1.063	0.870	1.023
Er	2.177	2.896		1.934		2.143		3.553		2.389	2.869	2.496	2.954
Tm	0.378	0.515		0.350		0.387		0.595		0.364	0.426	0.418	0.494
Yb	2.387	3.356		2.315		2.512		3.575		2.021	2.272	2.510	2.993
Lu	0.377	0.536		0.376		0.406		0.556		0.286	0.317	0.384	0.459
$(La/Yb)_N$	5.2	4.0		5.9		5.4		2.0		0.5	0.3	1.4	2.1
$^{87}Sr/^{86}Sr$	0.70463(2)											0.70455(2)	

Major element data are reported volatile-free and normalized to 100 %; FeO tot, total Fe as FeO; LOI, loss on ignition.
* Major-element data for rocks of the Higashi Formation is taken from Shinjo *et al.* (1990).
$(La/Yb)_N$ is chondrite-normalized La/Yb ratio. Uncertainties in Sr isotope ratios are 2σ mean (fifth digit).

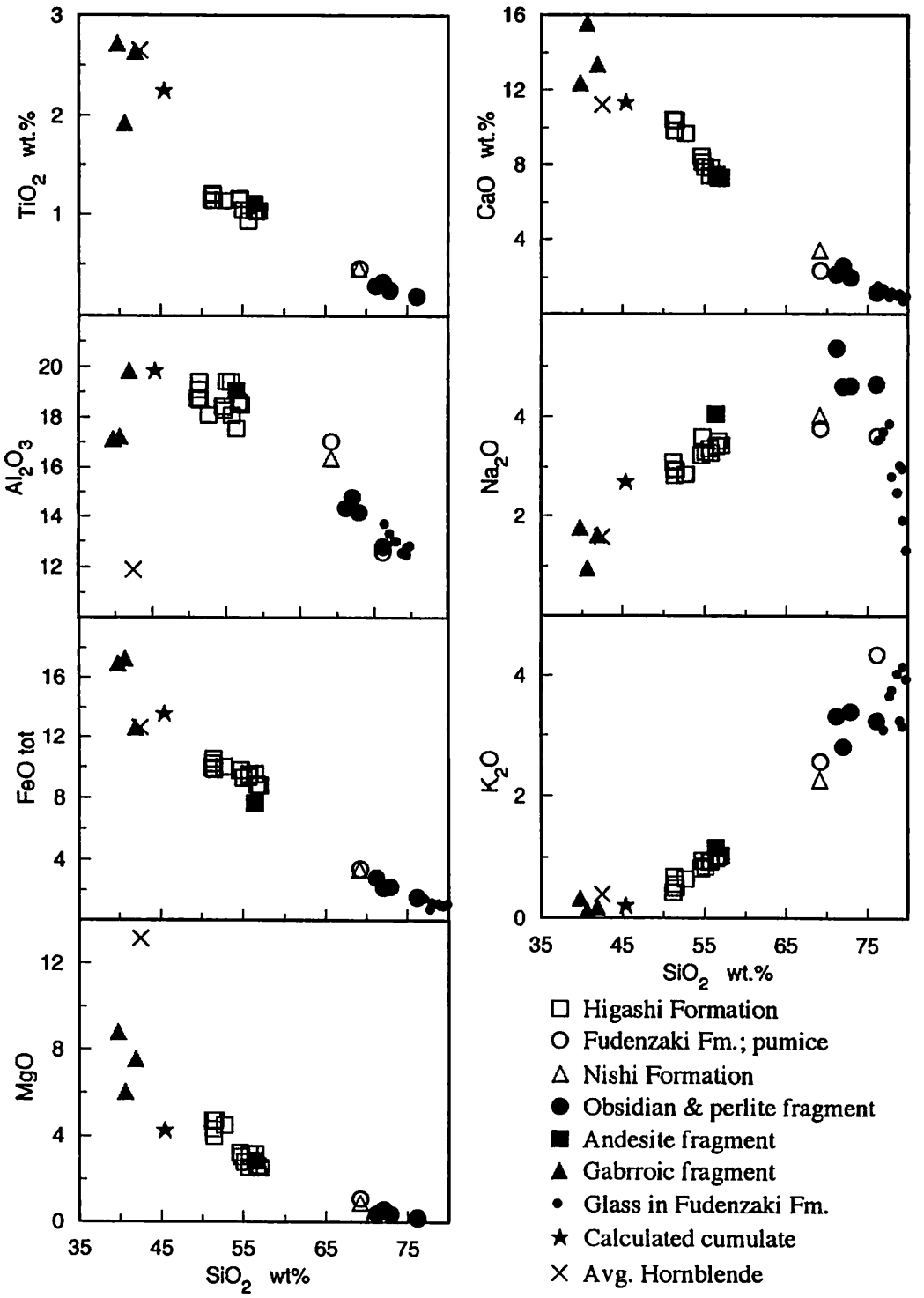

Fig. 7. Major oxides versus wt.% SiO_2 variation diagram for volcanic rocks and gabbroic fragments from the Aguni Group.

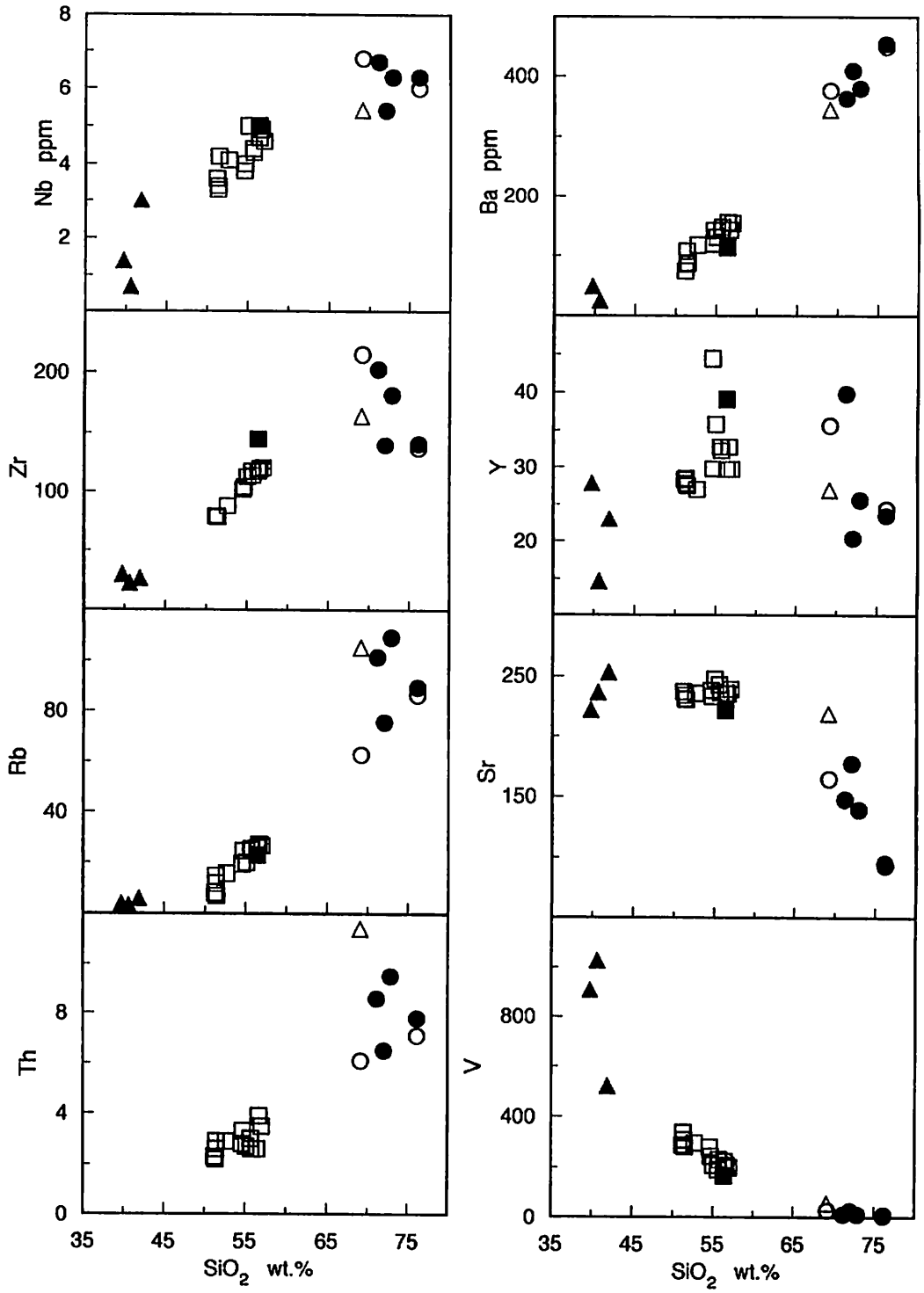

Fig. 8. Trace element versus wt.% SiO_2 variation diagram. Symbols are the same as in Fig. 7.

Table 3. Microprobe analyses of glass. Oxides are normalized to total 100 %.

	Fudenzaki Fm.; tuff		pumice		Obsidian & perlite fragments				
	A	C-1	A	C-1	A		C-1		
Sp. No.	AG8	AG12	AG24	AG25	AG48	AG49	AG65	AG68	AG69
	n=3	n=4	n=2	n=4	n=5	n=6	n=5	n=5	n=5
SiO_2	77.79	79.45	77.07	78.78	79.40	76.40	79.86	78.05	79.08
Al_2O_3	13.01	12.76	13.31	12.55	12.47	13.72	12.82	13.00	12.56
FeO tot	0.72	0.95	1.43	1.11	0.99	1.49	1.08	1.17	0.96
CaO	0.97	0.78	1.41	1.07	1.04	1.56	0.99	1.22	1.14
Na_2O	3.86	1.91	3.69	2.47	2.96	3.53	1.31	2.80	3.02
K_2O	3.66	4.14	3.09	4.02	3.15	3.31	3.94	3.75	3.24

while the suite is a medium-K series (Gill, 1981). Silica content is 69 wt.% for dacite from the Nishi Formation. The pumices in the Fudenzaki Formation have silica contents of 69 and 76 wt.%. Glasses are most enriched in SiO_2 and K_2O, and depleted in Al_2O_3, FeO total, and CaO.

The volcanic rocks of Aguni Group range from basalt to rhyolite, and have a pronounced compositional gap between 57 and 69 wt.% SiO_2. Note the near colinearity of basalt, andesite, and dacite on this plot. The composition of obsidian, perlite, and dacite fragments are within the range of pumice and dacite from the Fudenzaki and Nishi Formations. Scattered variation of Na_2O for felsic rocks would result from alkali mobility during the hydration of glass. An andesite fragment has a similar composition to andesite from the Higashi Formation. The felsic rocks are enriched in Na_2O, K_2O, Nb, Zr, Rb, Th, and Ba, whereas TiO_2, Al_2O_3, FeO total, MgO, CaO, Sr, V, and Cr are declined with increasing SiO_2. The gabbroic fragments generally lie on the SiO_2-poor extent of the trend.

Rare Earth Elements (REEs): Leedey chondrite normalized REE patterns for the igneous rocks from the Aguni Group are shown in Fig. 9. REEs for representative basalt and andesite from the Higashi Formation are also analyzed and the results are included in Table 2. The basalt and andesite of the Higashi Formation have slightly light REE-enriched REE patterns, with chondrite-normalized La/Yb ratio, $(La/Yb)_N$, ranging 1.4 to 2.1. The fresh andesite fragment in the Fudenzaki Formation is similar in shape and abundance to an andesite of the Higashi Formation. The REE patterns of felsic rocks differ from those of the basalt-andesite suite, crossing the basalt-andesite REE patterns. REE abundances of felsic rocks are light REE-enriched and strongly fractionated ($(La/Yb)_N$=4.0 to 5.9). Small negative Eu anomalies are present in the dacite-rhyolite suite, but not in the basalt-andesite suite. Within the dacite-rhyolite suite, concentrations of total REE decrease with increasing SiO_2 contents. The heavy REE concentrations decrease somewhat in rhyolite. The gabbroic fragments, on the other hand, have convex light REE-depleted REE patterns ($(La/Yb)_N$=0.3-0.5). The light REE concentrations are low, but middle to heavy REE contents are within the compositional range of volcanic rocks.

Sr-isotope data: All available data on Sr isotope ratios from volcanic rocks and fragments from the Aguni Group are plotted in Fig. 10. $^{87}Sr/^{86}Sr$ in samples from the Higashi Formation varies from 0.70452 to 0.70466 (Shinjo *et al.*, 1990). The dacite of the Nishi Formation has a Sr isotopic ratio of 0.70463, which is within the range of the basalt-

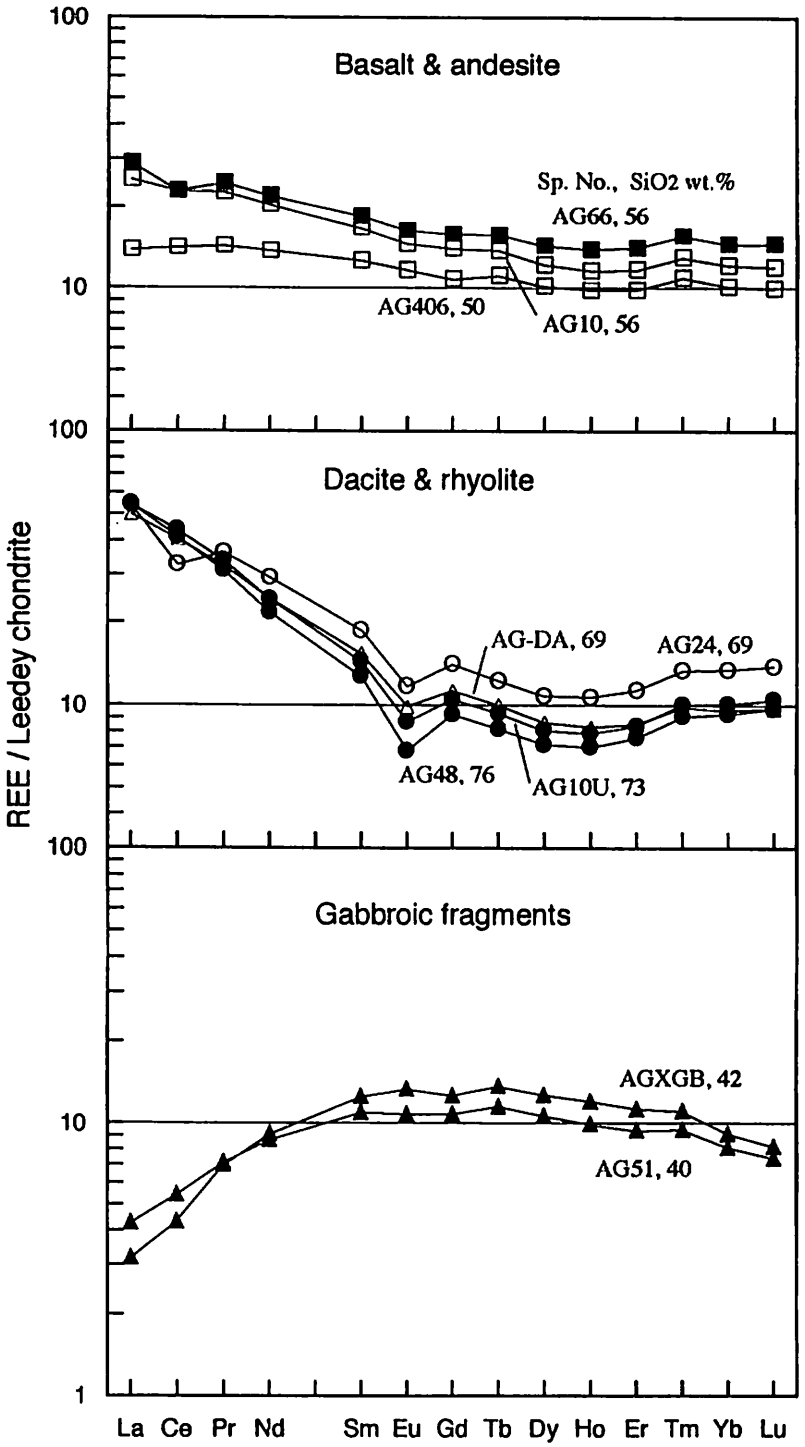

Fig. 9. Chondrite-normalized REE patterns for the volcanic rocks and gabbroic fragments of the Aguni Group. Normalizing values are taken from Masuda (1975) and Masuda *et al.* (1973).

andesite suite. The gabbroic fragment in the Fudenzaki Formation has a similar $^{87}Sr/^{86}Sr$ ratio of 0.70455 to those of the basalt-andesite suite as well.

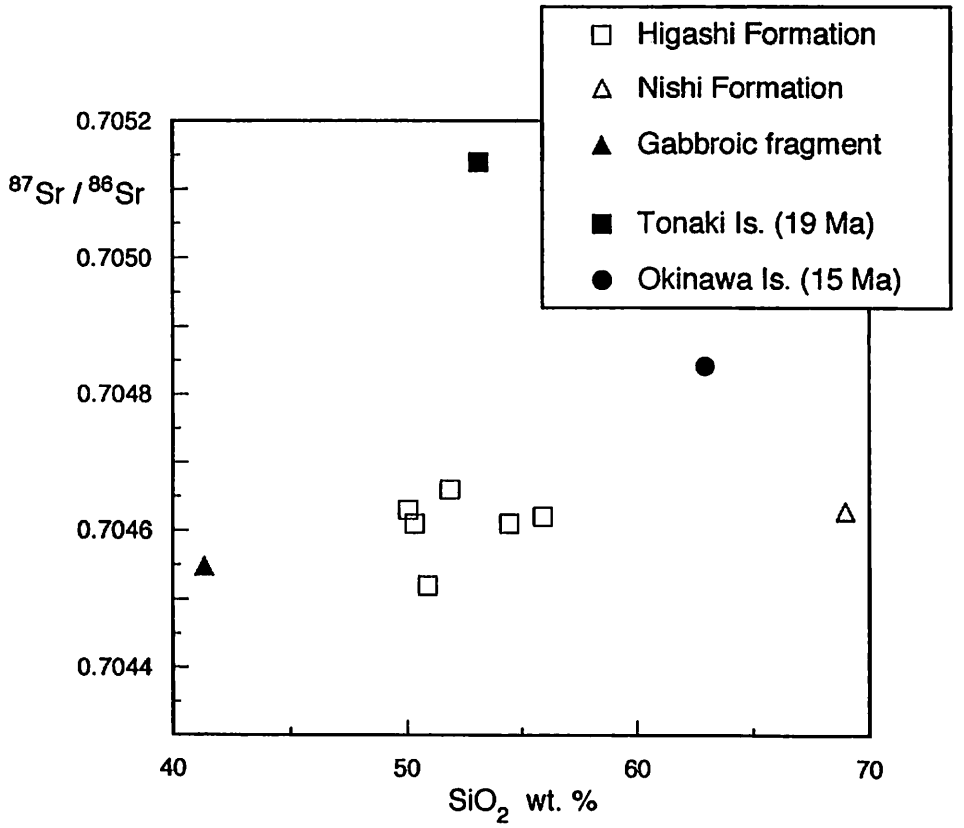

Fig. 10. $^{87}Sr/^{86}Sr$ ratios and wt.% silica for the volcanic rocks and gabbroic fragments from the Aguni Group. Sr isotopic ratios of a granodiorite (19 Ma) from Tonaki Island and a andesite dike (15 Ma) from Okinawa Island are also shown for comparison (Shinjo, unpubl.).

Discussions

1. Petrogenesis of the felsic rocks

The primary question we wish to address is whether the dacite and rhyolite magmas of the Aguni Group were melted from the crust or were derived from a basaltic precursor by fractional crystallization. In general, the isotopic compositions of volcanic rocks provides information on the origin of the magma's components, and the chemical composition and mineralogy place constraints on models of differentiation processes that occurred within the magma chambers.

On the basis of the mineralogy, Sr isotopic ratios, and incompatible element ratios of the basalt-andesite suite from the Higashi Formation, Shinjo *et al.* (1990) concluded that the andesites were produced by fractional crystallization of Plag + Cpx + Mt ± Olivine (Oliv) ± Opx from the basalt magma. The REE patterns of the basalt and andesite (Fig. 9) clearly confirm their suggestion.

The felsic fragments such as obsidian and perlite in the Fudenzaki Formation have similar mineralogy, major- and trace-element compositions, and REE patterns to the volcanic rocks of the Nishi and Fudenzaki Formation. These fragments might be related and represent products of earlier activity before eruption of the dacite of the Nishi Formation.

Initial $^{87}Sr/^{86}Sr$ ratio for a dacite lava (0.70463) is compatible to those for basaltic and andesitic lavas (0.70452-0.70466; n=6) and indicates that contamination of magma chamber(s) by radiogenic crustal rocks was not a significant factor in the evolution of the felsic magma. Thus the dacite and rhyolite would have been derived by closed-system fractional crystallization from mafic magma of andesitic composition. The felsic rocks have concave light REE-enriched REE patterns, with generally lower contents of middle to heavy REE compared to the basalt-andesite suite (Fig. 9). The presence of amphibole and pyroxene in the felsic rocks raises the possibility that the fractionation of those phases is responsible for lower middle to heavy REE contents, because the pyroxene/liquid and amphibole/liquid distribution coefficients for the middle to heavy REE (Irving, 1978) are significantly larger than for the light REE. A nagative Eu anomaly in the patterns of felsic rocks indicates fractionation of plagioclase. The behaviour of P_2O_5 can be reconciled with fractionation of accessory apatite, which have low solubilities in non-peralkaline felsic liquids (Watson, 1979).

We assumed that fractional crystallization from the andesite magma produced the dacites, and from this we performed the fractional crystallization model calculations, using the average compositions of andesite, dacite, and phenocrystic minerals (Table 4). Removal of Plag + Cpx + Amph + Mt + Ap in the weight proportions (57.2:7.3:23.7:11.4:0.3) reproduced the composition of a dacite after 57 % fractionation. The model suggests that the dacite formed through simple fractional crystallization of the andesite. Using results obtained from the above model and suitable partition coefficients (Fujimaki, 1986; Fujimaki *et al.*, 1984), we calculated REE pattern of evolved dacite magma. The calculated pattern is shown in Fig. 11 and is compared with average patterns of dacite, andesite, and gabbro. The calculated pattern of dacite is similar in shape to those of the actual dacite, while the middle to heavy REE abundances are higher in the calculated pattern. The calculated abundances of middle to heavy REE depend significantly on amphibole/liquid partition coefficients. Green and Pearson (1985) pointed out that the partition coefficients of REE ($D^{amph/liq}$) increase significantly with decreasing temperature and with bulk compositional change from basalt to rhyolite.

On the basis of the stratigraphy (Figs. 1 & 2), volcanic activities of the Aguni Group proceeded from dacite-rhyolite to basalt-andesite. It is highly unlikely that the andesite magma, parental to the felsic rocks, is identical with the andesite of the Higashi Formation. The model calculations require about 60 percent fractionation of andesite magma to produce felsic magma. If basaltic to andesitic magmas of the Higashi Formation are derived from a common magma chamber, their volume is expected to be limited because a high degree of fractionation is necessary to produce the felsic magma. Nevertheless, the amount of erupted mafic to intermediate magmas does not appear to be smaller than that of the felsic magma. Thus, we consider that basalt to andesite magma of the Higashi Formation had been derived from a newly generated magma chamber. Compositional and mineralogical similarities between the andesite fragment in the

Table 4. Result of least-squares, major-element modelling.

	Parent andesite		Daughter dacite	Mineral composition				
	obs.	calc.	avg.	Plag	Cpx	Amph	Mt	Ap
SiO_2	55.75	55.74	69.15	54.11	53.61	44.29	0.00	0.00
TiO_2	1.06	1.50	0.46	0.00	0.23	1.89	15.64	0.00
Al_2O_3	18.54	18.59	16.69	29.13	0.78	12.63	1.05	0.00
FeO tot	9.37	9.29	3.38	0.51	9.39	13.55	82.12	0.00
MnO	0.17	0.17	0.08	0.00	0.56	0.28	1.18	0.00
MgO	2.90	2.90	1.00	0.00	14.00	13.72	0.00	0.00
CaO	7.74	7.77	2.87	12.00	21.42	11.60	0.00	55.00
Na_2O	3.39	3.22	3.89	4.04	0.00	1.63	0.00	0.00
K_2O	0.94	1.15	2.40	0.20	0.00	0.42	0.00	0.00
P_2O_5	0.14	0.10	0.07	0.00	0.00	0.00	0.00	42.00

Sum of squars of residuals = 0.278

Phase		Fractions		Approx. modes of gabbroic fragments	
		wt. %	vol. %	AG51	AGXGB
Plag	0.330	57.2	48.5	60	45
Cpx	0.042	7.3	7.8	5	5
Amph	0.137	23.7	24.7	30	40
Mt	0.066	11.4	18.7	5	10
Ap	0.002	0.3	0.3		
Liquid	0.427				

Fudenzaki Formation and the andesite lavas from the Higashi Formation indicate that the andesitic precorsor for the felsic rocks would have been similar in composition to those of the Higashi Formation.

2. Gabbroic fragments and compositional gap between the andesites and dacites

Mafic crystal-rich inclusions provide information about fractionation processes occurring in the magmatic reservoir where the dacitic magma originated. The result of model calculations show that the mineral proportion calculated is generally in agreement with that observed in the gabbroic inclusions (Table 4). Moreover, $^{87}Sr/^{86}Sr$ ratio (0.70455) of a gabbroic fragment is within the range of the volcanic rock suite, impling that gabbroic fragments, Hbl-rich gabbros AG51 and AGXGB, are equivalent to cumulate involving the crystal fractionation from andesite to dacite. The REE patterns of gabbros also appear to coincide with the pattern of cumulate expected from the fractional crystallization. However, some discrepancies exist between the gabbroic fragment and the inferred cumulate for both major and trace elements. Judging from data distributions on Fig. 7, we consider the gabbroic fragments are slightly enriched in amphibole compared with the inferred cumulate. In summary, although several lines of evidence suggest that the gabbroic fragments are cumulates corresponding with the crystal fractionation, they do not directly represent cumulates from the andesite magma.

As previously mentioned, a compositional gap is present between the andesites and

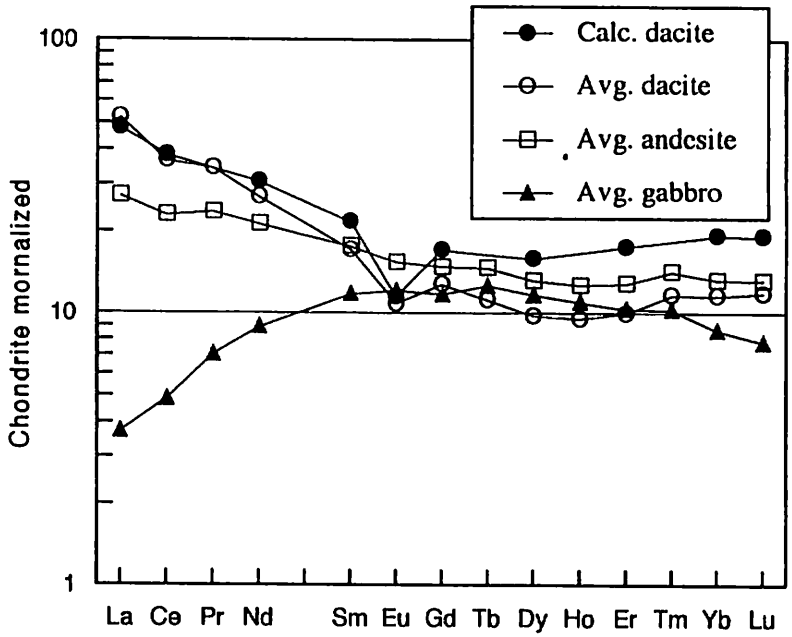

Fig. 11. Result of Rayleigh fractional-crystallization modelling compared with REE patterns of average andesite, dacite, and gabbroic fragment.

felsic rocks (Fig. 7). Similar compositional gap has been reported in volcanic rocks from Medicine Lake volcano (Grove and Donnelly-Nolan, 1986), where the compositional gap between andesite (57-62 wt.% SiO_2) and rhyolite (73-74 wt.% SiO_2) has been generated by low pressure fractional crystallization. Grove and Donnelly-Nolan (1986) pointed out that, at low pressure, experimentally produced Plag + Hbl + Opx + Mt or Plag + Cpx + Opx+Mt cotectics have shallow composition-temperature slope in the andesite-rhyolite range, and that the residual liquids produced over this part of the cotectic are less likely to be sampled than liquids on the evolved side where the composition-temperature slope steepens (Fig. 12). This indicates that a large percentage of crystals are removed over a small temperature range, evolved liquids are sampled, and a substantial amount of gabbroic cumulates are generated. In order to account for the compositional gap between andesite and dacite observed in the Aguni Group, we regard an analogous consideration as applicable. Since a large amount of crystallization occurs over a limited temperature range, a compositional gap develops. In practice, the obvious effect of fractionation of amphibole-bearing gabbroic assemblage is indicated by the REE patterns of the evolved felsic rocks.

Acknowledgments: We would like to thank Prof. H. Fujimaki at Tohoku University for helping us with Sr isotopic and XRF analyses. We are also indebted to Dr. R. van Woesik for his revision of the English and Dr. T. Oomori for his review of the original manuscript. This reseach was supported in part by the Uruma Fund and Fujiwara Natural History Foundation to R. Shinjo.

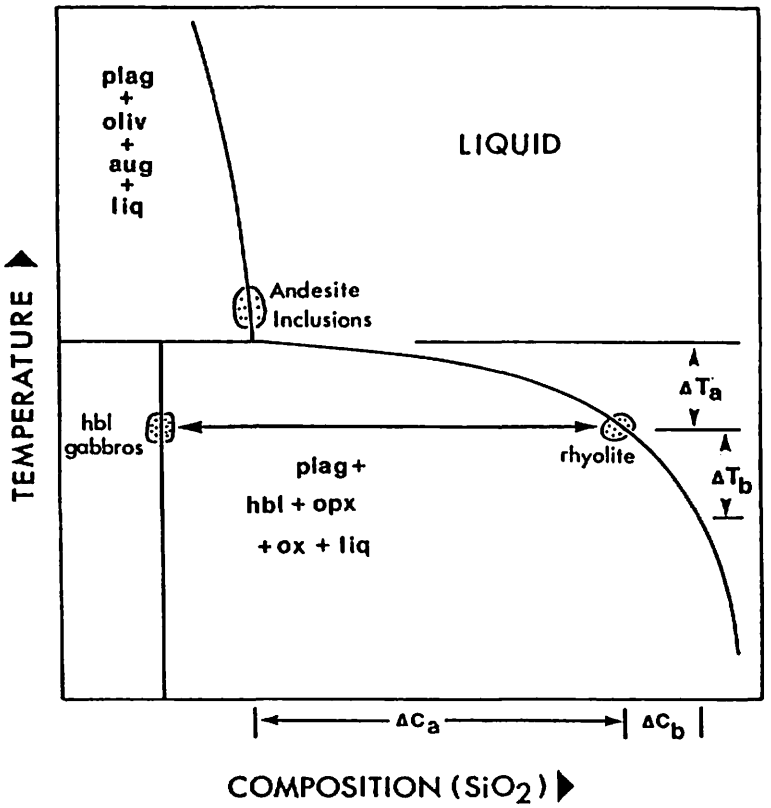

Fig. 12. Proposed temperature-composition (wt.% SiO_2 increases to right) diagram for late-stage crystallization at Medicine Lake volcano (Grove and Donnelly-Nolan, 1986). Initial crystallization of the amphibole-bearing assemblage resulting in a rapid change in composition (Δ Ca) in the residual liquid to rhyolite over a small temperature interval (Δ Ta), and results in a composition gap. Continued crystallization produces only a small change in the composition of residual liquid (Δ Cb) over a larger temperature interval (Δ Tb).

References

Daishi, M., M. Hayashi & Y. Kato, 1986. Fission track ages of some Cenozoic acidic intrusive rocks from Ryukyu Islands. *J. Japan. Assoc. Min. Petr. Econ. Geol.*, 81: 324-332 (in Japanese).

Fujimaki, H., 1986. Partition coefficients of Hf, Zr, and REE between zircon, apatite, and liquid. *Contrib. Mineral. Petrol.*, 94: 42-45.

Fujimaki, H. & K. Aoki, 1980. Determination of trace elements in rock samples by X-ray fluorescence. *J. Japan. Assoc. Min. Petr. Econ. Geol.*, 82: 411-414.

Fujimaki, H., M. Tatsumoto, & K. Aoki, 1984. Partition coefficients of Hf, Zr, and REE between phenocrysts and groundmass. *J. Geophys. Res.*, 89: B662-672.

Fujimaki, H., C. Wang, K. Aoki, & Y. Kato, 1992. Rb-Sr chronological study of the Hashigami plutonic mass, northern Kitakami, northeastern Japan. *J. Min. Petr. Econ.* Geol., 87: 187-196 (in Japanese).

Gill, J. B., 1981. Orogenic Andesites and Plate Tectonics. 390pp., Heidelberg, Springer-Verlag.

Green, T. H. & N. J. Pearson, 1985. Experimental determination of REE partition coefficients between amphibole and basaltic to andesitic liquids at high pressure. *Geochim. Cosmochim. Acta,* 49: 1465-1468.

Grove, T. L. & J. M. Donnely-Nolan, 1986. The evolution of young silicic lavas at Medicine Lake Volcano, California: Implications for the origin of compositional gaps in calc-alkaline series lavas.

Contrib. Mineral. Petrol., 92: 281-302.

Irving, A. J., 1978. A review of experimental studies of crystal/liquid trace element partitioning. *Geochim. Cosmochim. Acta*, 42: 743-770.

Kamiya, K., 1973. Geology of the Aguni-jima island. *Res. Papers, Okinawa Education Center*, 2: 18-31 (in Japanese).

Kato, Y., 1985. Aguni-jima island. *In*: Kizaki, K. ed.: Geology of the Ryukyu Islands, Okinawa Times Company: 115-118 (in Japanese).

Kuno, H., 1968. Differentiation of basaltic magmas. *In*: Hess, H. H. & A. Poldervaat, eds.: Basalts. 2: 623-688, John Wiley & Sons, Inc., New York.

Leake, B. E., 1968. A catalog of analyzed calciferous and subcalciferous amphiboles together with their nomenclature and associated minerals. *Geol. Soc. Am. Spec. Paper*, 98: pp.210.

Masuda, A. 1975. Abundances of monoisotopic REE, consistent with the Leedey chondrite values. *Geochem. J.*, 9: 183-184.

Masuda, A., N. Nakamura & T. Tanaka, 1973. Fine structures of mutually normalized rare earth patterns. *Geochim. Cosmochim. Acta*, 37: 239-248.

Shinjo, R. & Y. Kato, 1988. Petrography of the Ara-dake Formation, Kume-jima Island, the Ryukyu Islands. *J. Min. Petr. Econ. Geol.*, 83: 472-485 (in Japanese).

Shinjo, R., T. Hasenaka & H. Fujimaki, 1990. Petrology of volcanic rocks from the Higashi Formation in Aguni-jima island, central Ryukyus. *J. Min. Petr. Econ. Geol.*, 85: 282-297 (in Japanese).

Ujiié, H., 1983. Submarine geology west off the Okinawa Island in relation to the Ryukyu Arc development. *Memoirs Geol. Soc. Japan*, 22: 131-140 (in Japanese).

Watson, E. B., 1979. Apatite saturation in basic to intermediate magmas. *Geophy. Res. Pap.*, 6: 937-940.

Table A1. Representative microprobe analyses of plagioclases.

	Nishi Formation; dacite lava				Fudenzaki Formation; tuff				Fudenzaki Formation; pumice					
					A Member		C-1 unit		A Member			C-1 unit		
Sp. No.	AG74	AG74	AG74	AG76	AG8	AG8	AG12	AG12	AG24	AG24	AG24	AG25	AG25	AG25
	p. r.	p. c.	p. c.	p. c.	p. c.	p. c.	p. c.	p. c.	p. c.	p. c.	p. c.	p. c.	p. c.	p. c.
SiO_2	55.31	61.56	55.92	58.44	59.53	58.21	60.15	62.71	58.31	53.93	58.97	57.50	60.11	53.93
Al_2O_3	28.64	24.90	27.93	26.94	25.60	26.64	25.42	23.09	26.82	29.03	25.80	26.53	25.12	28.48
FeO	0.33	0.26	0.42	0.21	0.00	0.00	0.00	0.28	0.21	0.51	0.37	0.37	0.26	0.48
CaO	10.77	6.89	10.02	8.97	7.32	8.46	7.39	4.78	9.23	11.96	8.17	9.28	7.49	11.26
Na_2O	4.61	7.12	5.28	6.05	6.77	6.36	6.89	8.33	5.78	4.03	6.27	5.68	6.59	4.44
K_2O	0.32	0.61	0.32	0.40	0.38	0.36	0.38	0.55	0.31	0.20	0.32	0.29	0.39	0.26
Total	99.98	101.34	99.89	101.01	99.60	100.03	100.23	99.74	100.66	99.66	99.90	99.65	99.96	98.85
An	55.3	33.6	50.2	44.0	36.5	41.5	36.4	23.3	46.0	61.3	41.1	46.6	37.7	57.4
Or	1.9	3.5	1.9	2.3	2.3	2.1	2.3	3.2	1.8	1.2	1.9	1.8	2.3	1.6
	Obsidian and perlite fragments								Gabbroic fragments					
	A Member				C-1 unit									
Sp. No.	AG48	AG48	AG49	AG49	AG65	AG68	AG68	AG69	AG47	AG47	AG51	AG51	AG51	AG75
	p. c.	p. c.	p. c.	p. c.	p. c.	in xenolith	p. c.	p. c.	l. c.	in rind	l. c.	interstitial	l. c.	l. c.
SiO_2	60.82	57.13	56.19	53.46	58.67	46.78	46.26	56.67	46.49	49.25	45.37	54.77	53.15	45.84
Al_2O_3	24.64	27.68	26.85	28.72	27.46	34.08	33.36	28.47	33.78	31.77	33.93	28.12	28.12	35.00
FeO	0.23	0.29	0.33	0.38	0.38	0.77	0.86	0.25	0.58	0.89	0.61	1.00	1.04	0.49
CaO	6.87	9.68	9.87	11.99	8.39	17.30	17.11	10.13	18.24	15.70	18.22	11.64	12.54	17.95
Na_2O	7.24	5.49	5.54	4.04	6.74	0.76	0.98	4.32	0.88	2.12	0.64	4.16	3.68	0.57
K_2O	0.43	0.23	0.31	0.29	0.33	0.14	0.19	0.27	0.18	0.20	0.10	0.32	0.30	0.15
Total	100.23	100.50	99.09	98.88	101.97	99.83	98.76	100.11	100.15	99.93	98.87	100.01	98.83	100.00
An	33.5	48.7	48.7	61.0	40.0	91.8	89.5	55.4	91.0	79.4	93.4	59.6	64.1	93.7
Or	2.5	1.4	1.8	1.8	1.9	0.9	1.2	1.7	1.1	1.2	0.6	2.0	1.8	1.0

p. c.=phenocryst core; p. r.=phenocryst rim; l. c.=large crystal. A complete list of analyses can be obtained from the first author.

Table A2. Representative microprobe analyses of pyroxenes.

	Nishi Formation		Fudenzaki Formation; tuff						pumice		Obsidian & perlite fragments			
			A Member						A Mbr.	C-1 unit	A Mbr.		C-1 unit	
Sp. No.	AG74	AG76	AG8	AG8	AG8	AG12	AG12	AG12	AG24	AG25	AG48	AG49	AG68	AG69
SiO_2	53.09	52.83	51.72	51.82	53.53	53.19	54.69	53.13	53.28	51.75	53.09	52.79	54.14	53.25
TiO_2	0.14	0.16	-	-	-	-	-	-	-	-	-	-	0.17	0.15
Al_2O_3	0.65	0.32	-	-	-	-	-	-	-	-	-	-	0.20	0.09
FeO	28.26	28.11	31.69	31.07	25.16	25.06	22.09	28.49	25.95	28.28	29.19	26.29	21.91	24.94
CaO	1.43	1.31	1.50	1.62	1.17	1.65	1.22	1.78	1.81	1.93	1.86	1.05	1.12	1.85
Na_2O	17.04	17.38	14.89	15.45	19.70	19.71	22.52	17.78	18.80	16.62	17.33	18.96	22.1	19.59
K_2O	0.81	0.65	1.13	1.01	1.33	0.73	1.02	0.90	0.95	0.83	0.86	1.06	1.03	0.75
Total	101.42	100.76	100.93	100.97	100.89	100.34	101.54	102.08	100.79	99.41	102.33	100.15	100.67	100.62
Fs	47.4	46.9	53.1	51.9	40.6	41.0	34.8	46.5	42.8	48.0	47.7	42.8	35.0	41.0
En	50.9	51.7	44.5	46.0	56.7	57.5	63.2	51.7	55.2	50.2	50.5	55.0	62.9	57.4
Wo	1.7	1.4	2.4	2.2	2.8	1.5	2.1	1.9	2.0	1.8	1.8	2.2	2.1	1.6

	Obsidian & perlite fragments			Gabbroic fragments										
	A Member													
Sp. No.	AG68	AG68	AG68	AG47	AG47	AG47	AG51	AG51	AG51	AG51	AG75	AG75	AG75	AG75
SiO_2	52.47	52.80	52.59	49.18	51.04	49.96	50.27	49.60	51.77	50.74	50.78	51.60	51.26	51.83
TiO_2	0.18	0.23	0.29	1.22	0.76	0.82	0.58	0.79	0.47	0.56	0.70	0.56	0.55	0.52
Al_2O_3	0.78	0.77	1.20	5.19	3.36	4.17	3.26	3.92	2.32	2.84	3.07	2.54	2.52	2.66
FeO	8.73	9.25	9.49	9.78	8.04	8.48	8.11	8.51	7.68	7.88	8.27	8.55	8.39	9.48
CaO	0.55	0.55	0.58	0.30	0.23	0.32	0.25	0.25	0.22	0.24	0.36	0.40	0.30	0.45
Na_2O	13.81	13.79	13.54	13.63	14.56	13.77	13.67	13.15	14.52	14.09	13.82	13.98	13.73	13.65
K_2O	21.08	21.10	21.12	20.30	21.71	21.20	21.51	21.16	21.23	21.06	20.91	20.92	21.05	20.95
Total	97.60	98.49	98.81	99.60	99.70	98.72	97.65	97.38	98.21	97.41	97.91	98.55	97.80	99.54
Fs	14.5	15.2	15.6	16.3	13.0	14.1	13.5	14.4	12.6	13.1	13.9	14.2	14.0	15.6
En	40.8	40.4	39.8	40.4	42.0	40.8	40.6	39.7	42.6	41.9	41.3	41.3	40.9	40.1
Wo	44.7	44.4	44.6	43.3	45.0	45.1	45.9	45.9	44.8	45.0	44.9	44.5	45.1	44.2

Table A3. Representative microprobe analyses of amphiboles.and from results of Shinjo et al. (1990), we present a petrogenetic model on the volcanic rocks of the Aguni Group.

	Nishi Formation; dacite lava			Fudenzaki Formation; tuff						Obsidian & perlite fragments		
				A Member		C-1 unit		pumice A Member				
Sp. No.	AG74	AG74	AG76	AG8	AG8	AG12	AG12	AG24	AG24	AG49	AG69	AG69
SiO_2	46.88	45.54	46.73	45.22	44.07	48.59	48.86	47.38	45.05	44.01	43.43	44.32
TiO_2	1.21	1.81	1.27	2.02	2.52	0.96	1.01	1.71	2.30	2.21	1.85	2.19
Al_2O_3	8.10	9.65	8.09	7.95	9.16	6.40	6.39	7.35	9.32	10.47	12.38	11.65
FeO	16.07	16.52	17.35	17.67	17.95	15.39	15.11	15.53	14.38	14.86	13.29	14.07
MnO	0.45	0.58	0.54	0.43	0.43	0.81	0.79	0.63	0.43	0.41	0.27	0.31
MgO	12.38	11.61	11.47	11.23	10.11	13.48	13.80	12.80	12.47	12.15	13.45	13.01
CaO	10.45	10.15	10.54	10.65	10.86	10.16	10.32	10.67	10.97	10.80	11.37	11.18
Na_2O	0.87	1.24	0.58	1.40	1.71	0.83	0.48	1.10	1.39	1.56	1.60	1.43
K_2O	0.46	0.49	0.47	0.48	0.56	0.31	0.25	0.34	0.33	0.37	0.41	0.29
Total	96.87	97.59	97.04	97.05	97.37	96.93	97.01	97.51	96.64	96.84	98.05	98.45
Mg#	0.579	0.556	0.541	0.531	0.501	0.609	0.619	0.595	0.607	0.593	0.643	0.622
	Obsidian & perlite fragments				Gabbroic fragments							
Sp. No.	AG68	AG69	AG69	AG69	AG47	AG47	AG51	AG51	AG51	AG75	AG75	AG75
SiO_2	42.03	49.38	49.36	49.56	42.41	41.69	41.38	41.96	42.22	43.47	43.46	42.46
TiO_2	1.61	1.02	1.15	1.22	3.07	3.06	2.68	2.63	2.91	2.56	2.62	2.93
Al_2O_3	13.13	6.18	6.59	6.28	12.76	12.61	12.52	12.57	12.43	11.90	12.36	12.37
FeO	15.69	14.44	14.49	14.64	11.87	12.17	12.29	12.04	11.62	13.05	12.00	11.83
MnO	0.19	0.56	0.65	0.53	0.21	0.24	0.20	0.15	0.16	0.24	0.31	0.29
MgO	11.31	14.05	13.99	14.55	13.86	13.64	12.94	13.14	13.62	13.07	13.42	13.19
CaO	11.12	10.34	10.60	10.76	12.11	11.90	11.49	11.77	11.54	11.33	11.26	11.20
Na_2O	1.35	0.73	0.50	0.34	1.69	1.83	1.51	1.72	1.30	1.72	2.06	1.98
K_2O	0.42	0.29	0.25	0.32	0.51	0.55	0.52	0.47	0.46	0.34	0.33	0.37
Total	96.85	96.99	97.58	98.20	98.49	97.69	95.53	96.45	96.26	97.68	97.82	96.62
Mg#	0.562	0.634	0.632	0.639	0.675	0.666	0.652	0.660	0.676	0.641	0.666	0.665

Mg#=Mg/(Mg+Fe)